Neurobiology of Disease 124 (2019) 297–310

Contents lists available at ScienceDirect

Neurobiology of Disease

journal homepage: www.elsevier.com/locate/ynbdi

Tryptophan 32 mediates SOD1 toxicity in a in vivo motor neuron model of ALS and is a promising target for small molecule therapeutics

Michèle G. DuVal[a], Vijaya K. Hinge[b,c], Natalie Snyder[a], Richard Kanyo[a,d], Jenna Bratvold[a], Edward Pokrishevsky[e], Neil R. Cashman[e], Nikolay Blinov[b,c], Andriy Kovalenko[b,c], W. Ted Allison[a,d,f,*]

[a] Department of Biological Sciences, University of Alberta, Edmonton, AB T6G 2E9, Canada
[b] Nanotechnology Research Centre, Edmonton, AB T6G 2M9, Canada
[c] Department of Mechanical Engineering, University of Alberta, Edmonton, AB T6G 1H9, Canada
[d] Centre for Prions and Protein Folding Diseases, University of Alberta, Edmonton, AB T6G 2M8, Canada
[e] Djavad Mowafaghian Centre for Brain Health, University of British Columbia, Vancouver, BC V6T 2B5, Canada
[f] Department of Medical Genetics, University of Alberta, Edmonton T6G 2H7, Canada

ARTICLE INFO

Keywords:
[Cu-Zn] superoxide dismutase 1
Protein misfolding
Prion-like disease
Neuromuscular disease
Amyotrophic lateral sclerosis
Zebrafish
Uracil
Therapeutic
Nucleoside

ABSTRACT

SOD1 misfolding, toxic gain of function, and spread are proposed as a pathological basis of amyotrophic lateral sclerosis (ALS), but the nature of SOD1 toxicity has been difficult to elucidate. Uniquely in SOD1 proteins from humans and other primates, and rarely in other species, a tryptophan residue at position 32 (W32) is predicted to be solvent exposed and to participate in SOD1 misfolding. We hypothesized that W32 is influential in SOD1 acquiring toxicity, as it is known to be important in template-directed misfolding. We tested if W32 contributes to SOD1 cytotoxicity and if it is an appropriate drug target to ameliorate ALS-like neuromuscular deficits in a zebrafish model of motor neuron axon morphology and function (swimming). Embryos injected with human SOD1 variant with W32 substituted for a serine ($SOD1^{W32S}$) had reduced motor neuron axonopathy and motor deficits compared to those injected with wildtype or disease-associated SOD1. A library of FDA-approved small molecules was ranked with virtual screening based on predicted binding to W32, and subsequently filtered for analogues using a pharmacophore model based on molecular features of the uracil moiety of a small molecule previously predicted to interact with W32 (5′-fluorouridine or 5'-FUrd). Along with testing 5'-FUrd and uridine, a lead candidate from this list was selected based on its lower toxicity and improved blood brain barrier penetrance; telbivudine significantly rescued SOD1 toxicity in a dose-dependent manner. The mechanisms whereby the small molecules ameliorated motor neuron phenotypes were specifically mediated through human SOD1 and its residue W32, because these therapeutics had no measurable impact on the effects of $UBQLN4^{D90A}$, EtOH, or tryptophan-deficient human $SOD1^{W32S}$. By substituting W32 for a more evolutionarily conserved residue (serine), we confirmed the significant influence of W32 on human SOD1 toxicity to motor neuron morphology and function; further, we performed pharmaceutical targeting of the W32 residue for rescuing SOD1 toxicity. This unique residue offers future novel insights into SOD1 stability and toxic gain of function, and therefore poses an potential target for drug therapy.

1. Introduction

Amyotrophic lateral sclerosis (ALS) is a devastating neuromuscular degenerative disease with an approximate 2/100,000 incidence, in which the motor neurons controlling musculature gradually degenerate, leading to loss of muscle control including swallowing and

Abbreviations: 5'-FUrd, 5′-fluorouridine; ALS, amyotrophic lateral sclerosis; E3 media, standard media for raising larval zebrafish; fALS, familial amyotrophic lateral sclerosis; FDA, United States Food and Drug Administration; GFP, Green Fluorescent Protein; hpf, hours post-fertilization; HTVS, high throughput virtual screening; PBSTw, phosphate buffered saline pH 7.4 with 0.1% Tween20; sALS, sporadic amyotrophic lateral sclerosis; SOD1, [Cu, Zn] superoxide dismutase 1; $SOD1^{WT}$, wildtype SOD1; $SOD1^{W32S}$, SOD1 with missense mutation introduced (tryptophan to serine); TEER, Touch-Evoked Escape Response; Tel, telbivudine; U, Uridine; W32, residue #32 in SOD1 that is a tryptophan

* Corresponding author at: Department of Biological Sciences, University of Alberta, Edmonton, AB T6G 2E9, Canada.
E-mail address: ted.allison@ualberta.ca (W.T. Allison).

https://doi.org/10.1016/j.nbd.2018.11.025
Received 17 March 2018; Received in revised form 11 November 2018; Accepted 28 November 2018
Available online 04 December 2018
0969-9961/

respiration. [Cu−Zn] superoxide dismutase 1 (SOD1) was the first gene implicated in ALS and, although numerous other ALS associated genes have since been identified (including TDP43, FUS, C9ORF72), mutations in SOD1 remain prominent in familial cases (fALS, approx. 12%) and are found in a small number of sALS cases (approx. 1%) (Brown, 1993; Corcia et al., 2017). The human SOD1 protein, when mutated, has an increased propensity to misfold, and evidence of aggregates of misfolded SOD1 has been documented in cell culture, murine models, and tissues from patients with fALS (Bidhendi et al., 2016; Chia et al., 2010; Furukawa et al., 2013; Grad et al., 2015; Münch and Bertolotti, 2011; Sasaki et al., 2005; Sundaramoorthy et al., 2013; Wang et al., 2002; Yamagishi et al., 2007). SOD1 misfolding is likely impactful even in some sporadic ALS and non-SOD1 fALS, because misfolded SOD1 is observed in tissues from these patients (Bosco et al., 2011; Brotherton et al., 2012; Forsberg et al., 2010). The possibility of misfolded SOD1 inducing other SOD1 proteins to misfold in a prion-like manner is intriguing. However the nature of the prion-like SOD1 misfolding itself remains puzzling; unlike other protein misfolding paradigms, the characterization of physiologically relevant amyloid, fibrillization, or critical induction domains in the SOD1 protein has been limited (Banci et al., 2008; Didonato et al., 2003; Khan et al., 2017; Malinowski and Fridovich, 1979; Stathopulos et al., 2003), partly since mutations in SOD1 do not cluster at any part of the sequence. Further, how misfolded SOD1 exerts toxic effects remains even more perplexing, as mutant SOD1 model phenotypes may vary greatly based on mutation type and expression levels (Bruijn et al., 1997; Deng et al., 2006; Graffmo et al., 2013; Gurney et al., 1994; Jaarsma et al., 2008; Jonsson et al., 2006; Lemmens et al., 2007; Ramesh et al., 2010; Wong et al., 1995), and SOD1 loss-of-function models only partly recapitulate motor neuron dysfunction at best (Allison et al., 2017; Fischer et al., 2012; Ivannikov and Van Remmen, 2015; Muller et al., 2006; Reaume et al., 1996; Shi et al., 2014). However a particular residue may hold considerable sway in the misfolding and toxic properties of human SOD1 protein: residue 32, a tryptophan, which we will refer to as W32.

The W32 residue may be a prominent instigator in SOD1 misfolding and acquired toxicity. The induction or conversion of human wildtype SOD1 ($SOD1^{WT}$) protein to a misfolded state by mutant SOD1 protein has been demonstrated in ALS model mice and in cell culture. $SOD1^{G93A}$ induces $SOD1^{WT}$ to misfold and aggregate, leading to aggregates containing both proteins and accelerated disease progression in mice (Ayers et al., 2016; Bruijn et al., 1998; Deng et al., 2006; Wang et al., 2009). This interaction is further elaborated with evidence of $SOD1^{G127X}$ converting $SOD1^{WT}$ to the misfolded state in various cell lines; this interaction is suspected to be mediated by W32 (Grad et al., 2011). The influence of W32 on SOD1 conformation conversion appears significant, as mutation of this residue in $SOD1^{G93A}$ (in cultured motor neurons) (Taylor et al., 2007), $SOD1^{G127X}$, or $SOD1^{G85R}$ (in HEK-293 cells) (Grad et al., 2011) causes a dramatic reduction in their ability to misfold and convert $SOD1^{WT}$, thus reducing inclusions and cellular toxicity. The tryptophan at this residue is not well conserved, being serine in mice, and serine or threonine in many other non-primate vertebrates and invertebrates (Fig. 1A). Strikingly, W32 is the only tryptophan in human SOD1 (Grad et al., 2011), and this observation is amplified by noting tryptophan is not observed in any location of SOD1 among a diverse selection of other organisms (Dasmeh and Kepp, 2017). Thus we wanted to examine the relevance of W32 to the toxicity of SOD1 in an in vivo model.

As seen in many missense mutations, single residues can have considerable influence on the SOD1 monomer's overall stability, propensity to become misfolded, and to cause disease of varying severities and progressions; however it is striking to consider the possibility that W32 is especially influential upon SOD1 monomer's capacity to change the conformation of *other* monomers (Grad et al., 2011; Taylor et al., 2007). These findings are intriguing, as alteration of another monomer's conformation, i.e. conversion or template-directed misfolding, is a central criterion in prion-like propagation. Unique to the W32 residue is the discovery that mutating this tryptophan to a serine (W32S) as completed by Grad et al. (2011) leads to a reduction in overall misfolding and aggregation, making W32S the first SOD1 mutation with potentially beneficial effects, including ameliorating the toxicity of SOD1 (investigated herein). Tryptophan, despite being a hydrophobic residue, is solvent exposed on the third beta-strand of the SOD1 protein. Serine and threonine on the other hand are hydrophilic, which may offer more stability to the surrounding peptide. This may explain why residue 32 in SOD1 homologues of non-primate vertebrates is conserved for serine or threonine (Fig. 1A). Other residues evolutionarily unique to primates have been more closely studied, primarily for their contributions to SOD1 stability (especially at the dimer interface) leaving the question of W32 unaddressed (Dasmeh and Kepp, 2017).

We sought to validate the influence of this tryptophan residue on human SOD1 toxicity to axonal growth and motor neuron function in a disparate ALS animal model, the zebrafish, and to provide the first in vivo test of candidate small molecules that are predicted to act through interaction with W32 and thereby limit SOD1 acquired toxicity. Substitution of tryptophan for serine prevented SOD1 toxicity, thereby rescuing axonopathy and motor deficits; candidate drugs predicted to bind W32 likewise rescued these phenotypes in $SOD1^{WT}$-injected embryos. The W32 residue is thus influential in SOD1 toxicity in vivo, making it an attractive target for further development of therapeutic interventions.

2. Methods

2.1. Animal ethics statement

Husbandry and breeding of zebrafish for this study was approved under the protocol AUP00000077 by the Animal Care and Use Committee: BioSciences at the University of Alberta, under the auspices of the Canadian Council on Animal Care. Adult zebrafish were maintained according to standard procedures (Westerfield, 2000) in brackish water (1250 ± 50 μS) at 28.5 °C, and fed twice daily with either brine shrimp or trout chow.

2.2. Injecting Zebrafish with mRNA Encoding SOD1 and Drug Treatments

Human $SOD1^{WT}$, $SOD1^{G127X}$, and $SOD1^{W32S}$ were cloned into the pCS2+ vector via Gateway recombination for use in mRNA synthesis. The pCS2 + FLAG-UBQLN4 and pCS2 + FLAG-$UBQLN4^{D90A}$ vectors were gifted by Yongchao Ma and were recently described (Edens et al., 2017). Cloning mouse SOD1 was accomplished by ordering geneblocks from Integrated DNA Technologies (Skokie, IL) that were designed to encode NP_035564 (i.e $muSOD1^{WT}$, alongside a version encoding $muSOD1^{S32W}$) and included *attb* sites to allow Gateway cloning into pME and then pCS2+ vectors. Cloning of zebrafish SOD1 was similar, except that the pCS2 + $zfSOD1^{WT}$ vector was edited to create pCS2 + $zfSOD1^{S33W}$ by site-directed mutagenesis (QuikChange Lightning Site-Directed Mutagenesis Kit, Agilent Technologies) using following primers: Forward 5'-GAAAAGAAGCCAGTCAAGGTGTGGGGTG AAATTACTGGCCTTACT-3′ and Reverse: 5'-AGTAAGGCCAGTAATTTC ACCCCACACCTTGACTGGCTTCTTTTC-3′. Vectors were linearized with FastDigest *Not*I (Thermo Fisher, FD0593) and mRNA transcribed using the Ambion mMESSAGE SP6 transcription kit (Thermo Fisher, AM1340). mCherry mRNA and Tol2 mRNA (encoding a protein product that is innocuous to embryonic development) were produced similarly, for sorting injected embryos and for equilibrating total mRNA dosage between injection groups, respectively.

Embryos were collected from *mnx1:GFP* x AB crosses (ZFIN ID: ZDB-ALT-051025-4) (to visualize motor neurons with GFP) and injected with mRNA into the yolk at the 1–2 cell stage. Each embryo was injected with SOD1 mRNA at the doses indicated in the results, 100 pg mCherry mRNA, and a top-up of Tol2 mRNA (an innocuous product to normal zebrafish development), bringing the total mRNA dosage to

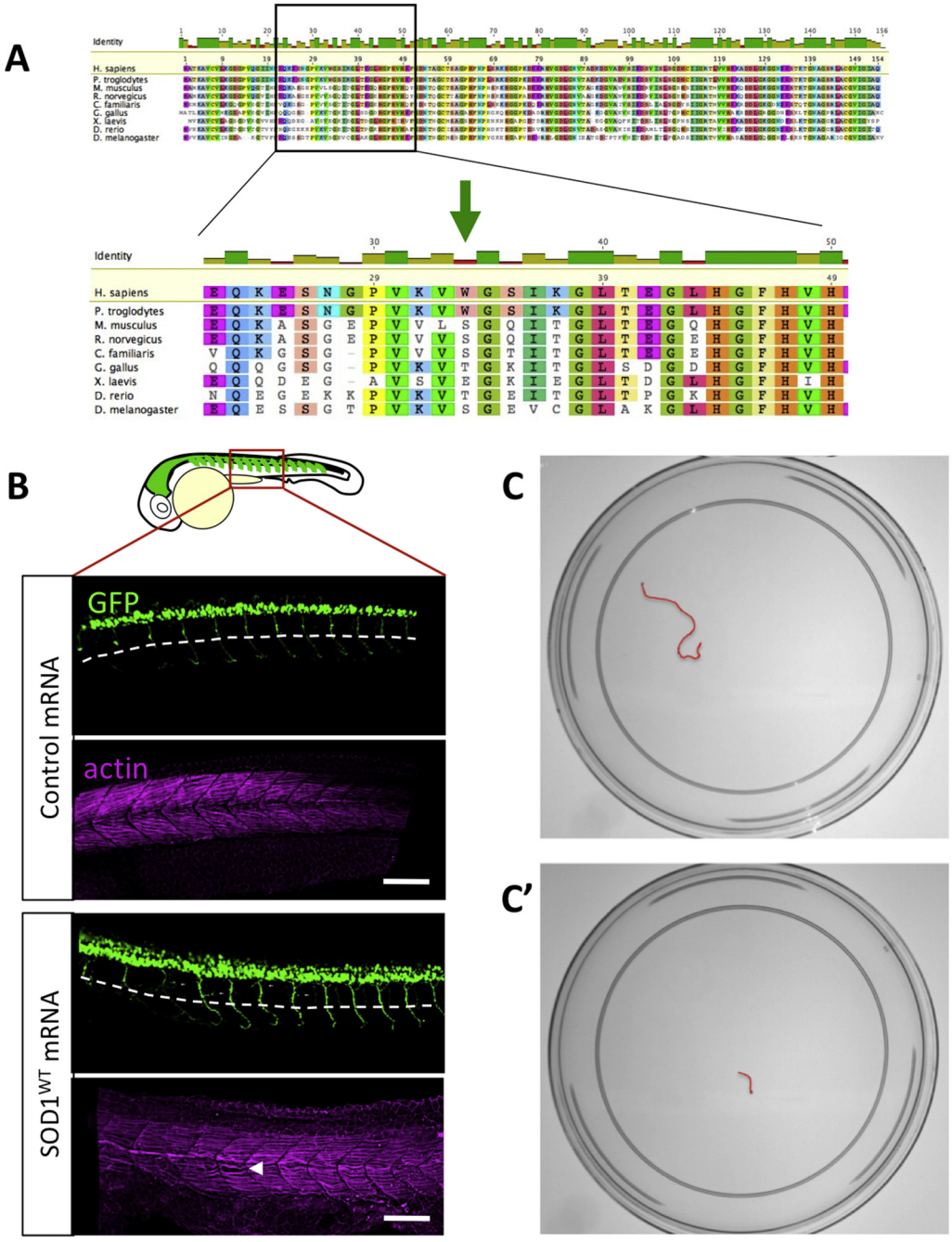

(caption on next page)

Fig. 1. $SOD1^{W32S}$ is less toxic than $SOD1^{WT}$ or a disease-associated mutant in vivo. A. SOD1 peptide sequence alignment showing that tryptophan at residue 32 in human SOD1 (green arrow) is not conserved at homologous residues in non-primates. B. Cartoon of a *mnx1:GFP* embryo (approx. 34 h post-fertilization) with GFP in the motor neurons (hindbrain, spinal cord) and motor neuron axons (exiting the spinal cord). Reconstructions of confocal images of embryo trunks (location depicted by inset) illustrate axons in a control mRNA injected embryo and abnormal axons ($SOD1^{WT}$ mRNA injected embryo). Individual primary axons exit the spinal cord and pass by the notochord (ventral notochord boundary indicated by white dashed line) to innervate the trunk muscles (phalloidin stain for muscle actin). In embryos injected with human $SOD1^{WT}$ and deleterious SOD1 mutants, abnormal primary axons have proximal branching (arrowheads) located above the ventral boundary of the notocord, a metric of axonopathy. Mild disruption of muscle fibres may be visible near abnormal axons (arrowhead). Scale bars 200 μm. C. Video stills of the Touch Evoked Escape Response (TEER) assay displaying recorded distance of a well-performing zebrafish larva, at 5.61 cm (C), and a poorly performing larva, at 1.43 cm (C′). D. Substituting residue W32 in human SOD1 ($SOD1^{W32S}$) significantly reduces axonopathy compared to human $SOD1^{WT}$ ($SOD1^{WT}$) and disease mutant human $SOD1^{G127X}$ ($SOD1^{G127X}$). $SOD1^{WT}$ and $SOD1^{G127X}$ cause more axonopathy compared to mRNA control injections ($p < .05$). E. Zebrafish embryos injected with $SOD1^{WT}$ or $SOD1^{G127X}$ mRNA swim a shorter total distance in the TEER assay compared to control mRNA injected fish ($p < .001$), but not embryos injected with $SOD1^{W32S}$ ($p = .89$) (Kruskall-Wallis test with Mann-Whitney pairwise comparisons). In subsequent TEER figures, one of two control mRNA values is displayed in each graph, indicating baseline control values obtained in experiments by one of two researchers who performed TEER assays. Data values that share matching grey letters within a figure panel are not significantly different. Embryo sample sizes noted below data points. (For interpretation of the references to colour in this figure legend, the reader is referred to the web version of this article.)

1900 pg. Thus the total mRNA dosage was normalized across all injection groups, including injecting combinations of SOD1 variants. Control mRNA groups were injected with 1800 pg Tol2 mRNA plus 100 pg mCherry mRNA. Following injection, embryos were maintained in E3 embryo media (Westerfield, 2000) at 28 °C with addition of PTU (Phenylthiourea, used to inhibit pigmentation) at approximately 10 h post-fertilization (hpf); at 24hpf they were sorted for mCherry fluorescence (indicating quality mRNA injection).

For 5′-fluorouridine (5'-FUrd), uridine (U), and telbivudine (Tel) treatments, drugs were mixed at the concentrations indicated, with 0.2% DMSO in E3 embryo media. Embryos were injected where indicated as described above, and at 12hpf dead embryos were removed and media replaced with drug-treated media. Vehicle control groups received 0.2% DMSO in embryo media. Embryos were maintained in drug media until fixation or use in Western blots or TEER assay.

2.3. Axonopathy assay

Embryos positive for GFP in the motor neurons were fixed at 34-36hpf in 4% paraformaldehyde for 40 min, then transferred to PBSTw (phosphate buffered saline pH 7.4 with 0.1% Tween20) until assessment. Axons of the primary motor neurons were scored for abnormal branching as per previous methods (Kabashi et al., 2010; Lemmens et al., 2007; Ramesh et al., 2010; Sakowski et al., 2012). In normal axon development, primary motor axons exit the spinal cord, extending past the notochord ventrally without branching, to innervate the trunk muscles. Axon branching at or before the notochord ventral boundary was scored as abnormal (Fig. 1B); the total number of abnormal branches was recorded for each embryo. Only embryos that lacked overt defects in development, body axis formation and patterning were assessed. Researchers were blinded to injection groups during axonopathy assessment.

2.4. TEER assay

The Touch-Evoked Escape Response (TEER) assay (Armstrong and Drapeau, 2013; Kabashi et al., 2011; Kabashi et al., 2010) was deployed to assess motor outputs of embryos that had been injected with mRNA as indicated and raised to 48-50hpf. Embryos screened positive for mCherry fluorescence and without gross body defects were selected for TEER. Each embryo was placed individually in the centre of a 14 cm diameter Petri dish, and touched on the tail with fishing line. The subsequent escape swims were recorded using a Basler aCA1300-60 g GigE camera (Basler AG, An der Srtusbek, Germany) (recording from directly above the dish) and analyzed in Ethovision XT (Noldus Information Technology Inc., Leesburg, USA). Videos were checked for successful tracking prior to analysis; those where the tracking function failed to detect or follow the embryo, or where the embryo failed to respond, were not analyzed. Video recordings were analyzed from the start of movement to the end, measuring for total swimming distance (Fig. 1C). Only embryos that lacked overt defects in development, body axis formation and patterning were assessed. Experimenters were blinded to treatment groups during the TEER assay and during video analysis.

2.5. Western blot and protein quantification

Embryos injected with $SOD1^{WT}$ and $SOD1^{W32S}$ mRNA at the dosages indicated were screened for mCherry fluorescence. At 30hpf embryos were sorted into biological replicates (five embryos per replicate), de-yolked with de-yolking buffer (Westerfield, 2000), washed with cold Ringer's solution, and homogenized by using a pestle and brief sonication in cell lysis buffer containing 20 mM HEPES, 0.2 mM EDTA, 10 mM NaCl, 1.5 mM $MgCl_2$, 20% glycerol, 0.1% Triton-X, and 0.5% Protease Inhibitor Cocktail Set III (Millipore, CA80053–852). Protein concentration was determined with Qubit® fluorometer (Invitrogen, Carlsbad, CA, USA) prior to SDS-PAGE. SDS-PAGE was set up as previously described (Kanyo et al., 2011) using a Mini-PROTEAN Tetra Cell (Biorad Labroratories, Inc., Herculas, CA, USA). Samples (20 μg of total protein/well) were loaded on a 12% gel and run in electrophoresis buffer (25 mM Tris, 190 mM glycine, 3.5 mM SDS). After electrophoresis, gels were equilibrated in Towbin's buffer (25 mM Tris, 190 mM glycine, 20% methanol) for 15 min and protein samples were transferred onto PVDF membrane at 100 V for 1 h.

Membranes were blocked in 5% dried skim milk dissolved in TBST (50 mM Tris, 150 mM NaCl, and 0.05% Tween 20, pH 7.5) for 1 h. SOD1 was detected with rabbit anti-SOD1 antibody (Enzo Life Sciences, ADI-SOD-100) at 1:10000 dilution. Actin was targeted with a rabbit anti-actin antibody (Sigma, A2066) at 1:1500. All antibodies (primary and secondary) were diluted in 5% skim milk/TBST. Membranes were incubated with primary antibodies overnight at 4 °C with gentle agitation. Immunoblots were washed in TBST (4 × 15-min) and probed with horse-radish peroxidase-conjugated anti-rabbit secondary antibody (1:1000 dilution; Jackson Immuno, 111–035-003) for 1 h at room temperature. Following washing in TBST as described above, SOD1 or actin was visualized using Pierce® ECL Western Blotting Substrate (Thermofisher, 32,106). Band intensity was measured via densitometry with ImageJ64 for Windows (Wayne Rasband, National Institutes of Health, USA; http://imagej.nih.gov/ij) and SOD1 was quantified by normalizing human SOD1 band intensities to actin band intensities.

2.6. Statistical analysis

Statistical analysis of axonopathy and TEER data was performed using Kruskall-Wallis tests with post-hoc Mann-Whitney pairwise comparisons in Stata/SE 14.1 for Mac (2015, StataCorp). Analysis of Western blot band intensity values was performed using one-tailed ANOVA with Dunnet's multiple comparisons in Prism 7 (GraphPad Software).

2.7. High throughput virtual and pharmacophore screening of FDA-approved drugs

The database preparation of FDA (United States Food and Drug Administration) approved compounds, receptor structure preparation, high throughput virtual and pharmacophore screening studies were performed with Molecular Operating Environment (MOE) (2013) integrated drug discovery package from Chemical Computing Group (CCG) Inc., (Montreal, Canada) (2018).

For preparation of the compound database, a library of 1861 FDA approved compounds was downloaded from Drugbank (version 5.0.1) (Wishart et al., 2006) in SDF chemical-data file format (www.drugbank.ca). The SDF format compounds were subjected for database preparation in MOE compatible format then used for the HTVS and pharmacophore screening studies. The preparation included importing SDF format compounds to MOE, removal of counterions and solvent molecules, protonation of compounds at pH = 7.0, and energy minimization. The detailed methodology of the protocols used for database preparation can be found in MOE documentation (2018).

For receptor structure preparation, atomic coordinates of the receptor (monomeric apo-SOD1 structure) were taken from the X-ray structure of the human SOD1 enzyme with 5'-FUrd ligand bound to its W32 binding site (PDB code 4A7S) (Wright et al., 2013). The hetero atoms were removed, and only the coordinates of the first SOD1 monomer were used to build the structural model of the receptor. The *Protonate3D* module of MOE was used to assign protonation states of polar amino acids at pH = 7.0. Hydrogen atom coordinates missed in the experimental structure were added with the *Protein Structure Preparation* module of the MOE package, and then partial charges were assigned to the receptor atomic sites. Once prepared as described, the above structure was optimized to relax strained geometry and possible steric clashes by using energy minimization with a gradient tolerance of 0.1 Kcal/mol/Å. For minimization, the Generalized Born Volume Integral (GB/VI) formalism and the Amberff10 force field were chosen from the Amber10:EHT option available with MOE.

High throughput virtual and pharmacophore screening was done with the *Dock module* in the MOE package for the HTVS studies, to screen the FDA approved compounds at W32 binding site. Residues from the W32 binding site of SOD1, in particular, Asn19, Phe20, Glu21, Gln22, Lys30, Val31, Trp32, Gly33, Ser34, Asp96, Val97, Ser98, Ile99 and Glu100 were selected as binding site residues for HTVS studies. All other residues within 5 Å distance were also included in the docking site definition for the *triangle matcher ligand placement* method. These are residues Ala1, Thr2, Lys3, Ala4, Val5, Cys6, Val7, Leu8, Lys9, Gln15, Gly16, Ile17, Ile18, Lys23, Glu24, Gly27, Pro28, Val29, Ile35, Lys36, Gly37, Gly93, Val94, Ala95, Asp101, Ser102, Val103, Ile104, Ser105, Leu106 and Ser107. The Amber10:EHT force field option available with MOE allowed us to assign the Amberff10 force field (Case et al., 2008) and EHT (extended Hückel theory) (Gerber and Muller, 1995) based parameters for the receptor and compounds, respectively. The atomic partial charges for the receptor assigned from Amberff10 force field (Case et al., 2008) and for the ligand AM1-BCC (Jakalian et al., 2000; Jakalian et al., 2002) method charges were assigned. 30 binding poses were generated for each compound from the database by using the *triangle matcher placement* method. These poses were scored with the London ΔG scoring function, and the top 5 poses were refined using *Rigid Receptor* method and finally rescored using GBVI/WSA ΔG scoring function. The pharmacophore model was built based on the molecular features of the uracil moiety of 5'-FUrd (Fig. 3C) (Wright et al., 2013). The model consists of hydrogen bond acceptor atoms from 4, 2 dioxy groups on uracil and aromatic features of pyrimidine ring. The built pharmacophore model was used to identify the uracil-like molecular features in FDA approved compounds obtained from HTVS docking studies. The detailed explanation of methodology and modeling tools used for screening can be found in the MOE package documentation (2018).

3. Results

3.1. Altering the W32 residue reduces SOD1 toxicity as measured by motor neuron axonopathy and function

The significance of the W32 residue to SOD1 toxicity in the central nervous system was tested in an in vivo ALS model of motor neuron morphology and function: zebrafish (Duval et al., 2014; Kabashi et al., 2010; Lemmens et al., 2007; Ramesh et al., 2010; Sakowski et al., 2012). Human SOD1 variants were delivered to zebrafish embryos as mRNA shortly after fertilization as per established methods (Lemmens et al., 2007). Injected embryos were then assessed for motor neuron axonopathy and swim performance, with comparisons to control injected groups.

Overexpression of human $SOD1^{WT}$ or fALS disease-associated SOD1 mutants has previously been shown to cause an increased frequency in primary motor neuron axonopathy (defined previously and here as primary axon branching occurring above the ventral boundary of the notochord- see Methods and Fig. 1B) compared to that of un-injected or control mRNA injected embryos. The magnitude of this phenotype correlates well with disease severity; we confirmed these past results and extend this trend by injection of $SOD1^{G127X}$, which is an aggressive clinical variant with fairly rapid progression (Andersen et al., 1997; Hansen et al., 1998; Jonsson et al., 2004; Kabashi et al., 2010; Lemmens et al., 2007; Ramesh et al., 2010). $SOD1^{G127X}$ induced 20% more axonopathy than $SOD1^{WT}$ and both these values were significantly increased from controls (34% increase in $SOD1^{WT}$ and 62% in $SOD1^{G127X}$ compared to mRNA controls) (Fig. 1D; $p < .05$), thus further confirming in our hands that penetrance of the axonopathy phenotype is a good predictor of disease severity for fALS SOD1 variants. We also assessed the impact of these variants on motor neuron function in zebrafish larvae using the Touch-Evoked Escape Response (TEER) (Armstrong and Drapeau, 2013; Kabashi et al., 2011; Kabashi et al., 2010), where a larva performs a burst of swimming upon being touched on the tail (Fig. 1C). Injecting $SOD1^{G127X}$ reduced swim performance 20% more than $SOD1^{WT}$, and both these groups had significantly decreased swim performance from control mRNA injected larvae (distances compared to mRNA controls were 38% and 50% lower in $SOD1^{WT}$ and $SOD1^{G127X}$ groups, respectively) (Fig. 1E; $p < .001$).

To assess if residue W32 has an impact on motor neuron deficits induced by human SOD1 overexpression, we engineered $SOD1^{W32S}$ mRNA and delivered it to zebrafish embryos. $SOD1^{W32S}$ injected embryos did not show any increase in axonopathy, in fact producing about half as many motor neuron defects on average compared to $SOD1^{WT}$ ($p < .001$) and even fewer compared to the ALS-associated mutant $SOD1^{G127X}$ (Fig. 1D). Also, in contrast to $SOD1^{WT}$ and $SOD1^{G127X}$, $SOD1^{W32S}$ injected larvae did not show impaired motor function, swimming a comparable distance to control larvae in response to a touch on the tail ($p = .89$) (Fig. 1D). These results support the hypothesis that residue W32 is important for induction of SOD1 cytotoxicity.

An alternative explanation for the significantly lower incidence of axonopathy in embryos injected with $SOD1^{W32S}$ might reside in the kinetics of the transcript or protein abundance: e.g. it is possible that injection of $SOD1^{W32S}$ led to lower levels of protein compared to $SOD1^{WT}$, despite great care to deliver equal doses via mRNA injection. To address this, we measured protein levels in triplicate samples of five 30hpf embryos injected with various mRNA doses of $SOD1^{WT}$ and $SOD1^{W32S}$. Human SOD1 protein (approx. 21 kDa) and the zebrafish endogenous Sod1 protein (approx. 17 kDa) were readily discriminated on Western blots (Fig. 2A, larger band absent in protein from uninjected larvae). Western blot analysis in fact reported lower $SOD1^{W32S}$ protein abundance compared to $SOD1^{WT}$ when equal amounts of SOD1 mRNA are injected. To ensure that the less severe phenotypes we observed in $SOD1^{W32S}$ compared to that of $SOD1^{WT}$ were not due to differences in SOD1 protein abundance, we adjusted the doses of mRNA delivered

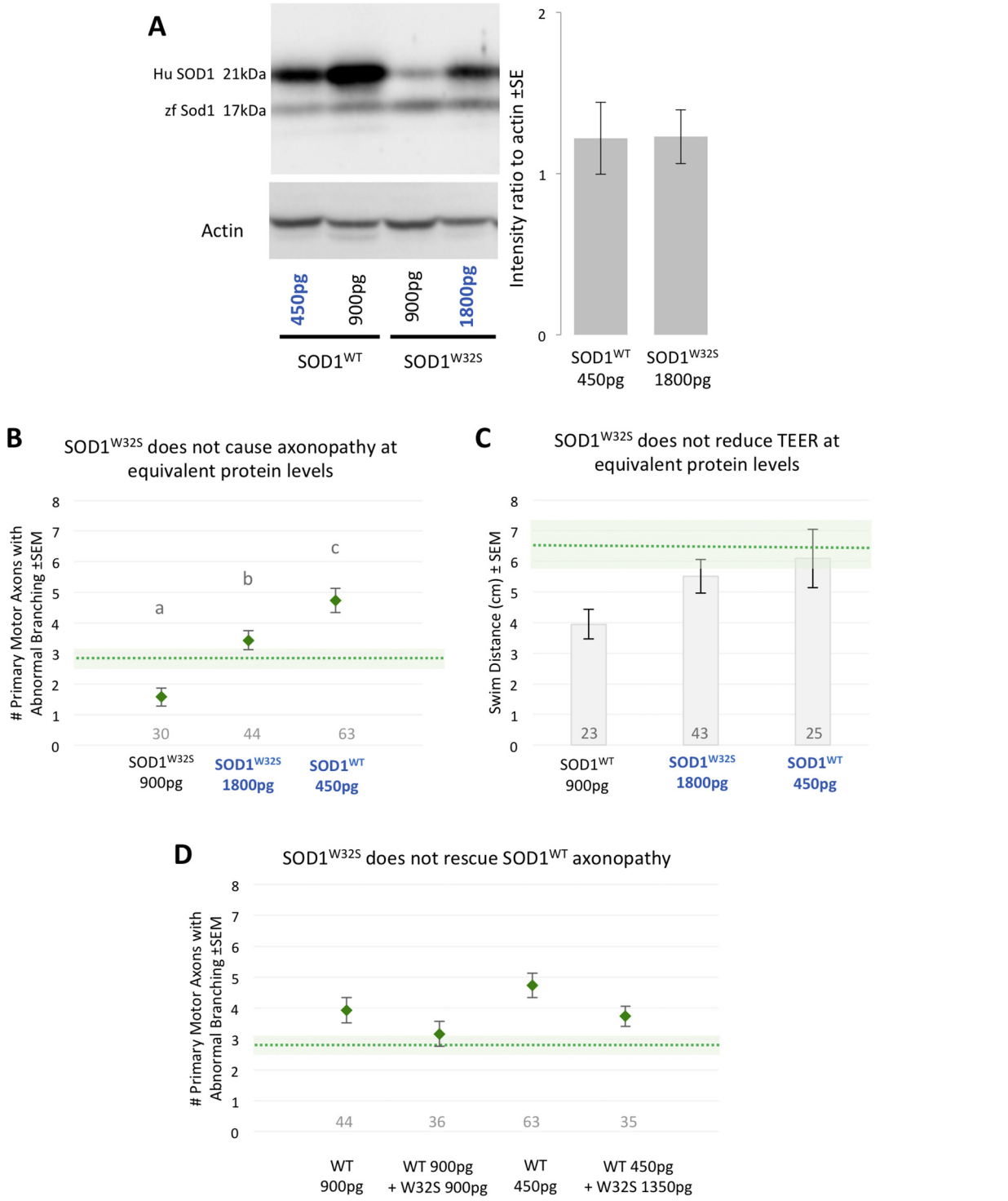

Fig. 2. At equivalent protein levels, SOD1^{W32S} does not cause a severe axonopathy phenotype compared to SOD1^{WT}. A. SOD1^{W32S} and SOD1^{WT} mRNA were injected at varying doses to determine equivalent protein levels as measured on Western blot (450 pg of WT and 1800 pg of W32S; equivalent protein groups highlighted in blue font; quantification shown for $n = 3$ biological replicates containing 10 embryos each). The immunodetection reveals both exogenous human SOD1 (Hu SOD1, band absent in uninjected larvae) and endogenous zebrafish Sod1 (zf Sod1). B. At 1800 pg, SOD1^{W32S} produces an increase in axonopathy over that of the 900 pg dose ($p < .001$), but this axonopathy was statistically insignificant compared to control mRNA axonopathy levels (mRNA control average shown as green dotted line with SEM in green shading) ($p = .07$). SOD1^{WT} at 450 pg produces significantly more axonopathy ($p < .001$). C. At 1800 pg, SOD1^{W32S} does not significantly reduce TEER compared to control mRNA groups (green line and shading, $n = 35$ embryos) ($p = .51$), and it is also not significantly different from TEER in SOD1^{WT} 450 pg-injected embryos ($p = .86$). D. SOD1^{W32S} was co-injected with SOD1^{WT} to determine if SOD1^{W32S} can rescue toxicity caused by SOD1^{WT}; while a mild rescue was seen at two dose combinations tested, this was not statistically significant. (Kruskall-Wallis test with Mann-Whitney pairwise comparisons). mRNA control average ± SEM for each experiment indicated as green dotted line and shaded box. Data values that share matching grey letters are not significantly different. Embryo sample sizes noted below data points. (For interpretation of the references to colour in this figure legend, the reader is referred to the web version of this article.)

such that the fish produce similar SOD1 protein abundance for each variant. Injection of 1800 pg of $SOD1^{W32S}$ mRNA resulted in an amount of protein similar to injection of 450 pg of $SOD1^{WT}$ mRNA (Fig. 2A). We assessed axonopathy and TEER at these doses. We found that, while axonopathy increased between 900 pg and 1800 pg mRNA doses of $SOD1^{W32S}$, it remained lower than axonopathy in 450 pg $SOD1^{WT}$ injected embryos and not significantly different from controls (control average and SEM indicated on graphs with green dotted line and green box respectively) (Fig. 2B; $p = .07$). Similarly, injection of 1800 pg of $SOD1^{W32S}$ caused a slight nonsignificant decrease in TEER compared to control mRNA ($p = .51$), and was also not significantly different from TEER in 450 pg $SOD1^{WT}$ embryos ($p = .86$) (Fig. 2C). Thus SOD1 harboring the W32S mutation does not induce significant axonopathy above control levels, even when presented as a large mRNA dose or a protein level equivalent to $SOD1^{WT}$. Further, W32 is apparently required for human SOD1 to induce motor neuron defects in this animal model, because when $SOD1^{W32S}$ protein was present in equal abundance to $SOD1^{WT}$ it continued to result in less axonopathy (Fig. 2B).

Alteration of the W32 residue may render the SOD1 monomer more stable and less vulnerable to templating of protein misfolding, or may act in *trans* to confer additional stability onto other monomers. For example, if $SOD1^{W32S}$ were to heterodimerize with a wildtype W32-containing counterpart, or a SOD1 dimer containing $SOD1^{W32S}$ were to interact with another SOD1 dimer, the interaction may reduce the probability of misfolding in the wildtype, W32-containing counterparts (Banerjee et al., 2016; Shi et al., 2016). To discern whether the W32S substitution confers a protective effect on neighbouring SOD1 proteins (i.e. if $SOD1^{W32S}$ can rescue $SOD1^{WT}$ and its toxicity), we co-injected $SOD1^{WT}$ with $SOD1^{W32S}$ at two different dosage ratios (900 pg each or 450 pg + 1350 pg, respectively). If $SOD1^{W32S}$ can reduce the toxic propensity of neighbouring monomers or dimers, we would predict it could rescue the $SOD1^{WT}$-induced axonopathy. We found a non-statistically significant rescue effect at both doses (Fig. 2D), which does not support the notion that a W32S substitution in SOD1 was able to prevent or reduce the cytotoxicity of other SOD1 monomers or proteins, or at least not to a significant degree. Thus the $SOD1^{W32S}$ protein has a lower propensity to become toxic, but within our model we did not find evidence that it substantially alters the neurotoxic properties of nearby wildtype (W32-containing) SOD1 proteins.

3.2. The W32 residue is a promising drug target to mitigate SOD1-induced motor neuron deficits

The presence of W32 may universally influence the human SOD1 protein's propensity to become unstable and misfolded, as seen by its effects in both wild type SOD1 and in various mutants (Grad et al., 2011; Taylor et al., 2007), thus W32 would be a desirable target to generally abate SOD1 misfolding and toxicity. 5′-fluorouridine (5'-FUrd) has been predicted to bind to the W32 residue (Wright et al., 2013) (Fig. 3A, B), and so we sought to test this small molecule in our zebrafish model. In addition to testing 5'-FUrd, we performed high throughput virtual screening (HTVS) using a pharmacophore model to identify new compounds which could bind at the W32 site of SOD1 and potentially inhibit SOD1 toxicity. The W32 residue is located on the surface of the β-sheet, is highly solvent exposed, and does not have a conventional binding pocket, therefore this site poses difficulties for designing new compounds. This can be overcome by filtering screened compounds through the pharmacophore model, using a template of a compound already confirmed to bind this site on SOD1. Initially, HTVS studies were performed with a library of FDA approved compounds at W32 site of SOD1. The X-ray crystallography study of Wright et al. (Wright et al., 2013) demonstrated that 5'-FUrd binds at the W32 residue of SOD1, and not at the SOD1 dimeric interface as proposed by previous reports (Nowak et al., 2010; Ray et al., 2005) (Fig. 3A, B). The molecular interaction features of the uracil moiety of 5'-FUrd at the W32 site were utilized to build the pharmacophore model (Fig. 3C). The library of FDA approved compounds from HTVS studies was further filtered through the pharmacophore model and 17 compounds were identified. Among these 17 compounds, ten compounds were selected based on their binding energy, π-π interactions ability with indole side chain of W32 residue, and similarity with 5'-FUrd (Supplemental Table 1).

Based on analysis of molecular descriptors of top ranked compounds, we selected telbivudine (Fig. 4, Ligand L5 in Supplemental Table 1), the blood brain barrier-permeable thymidine analogue used to treat Hepatitis B. Telbivudine impairs viral DNA replication through phosphorylation into telbivudine triphosphate and being incorporated into viral DNA, which terminates elongation. It does not inhibit human polymerases, and it is not incorporated into human DNA. Telbivudine has a good drug safety profile, though with the caveats of myopathy and peripheral neuropathy rarely documented in some patients, and axonopathy (causation inconclusive) at high doses in animal toxicity studies; the mechanisms behind these side effects have not been elucidated (Bridges et al., 2008; Fung et al., 2011; Zhang et al., 2008). Neither uridine nor telbivudine have been tested for rescuing the effects of SOD1 toxicity in an animal model.

We proceeded to test 5'-FUrd, uridine, and telbivudine as therapeutics against $SOD1^{WT}$-induced motor neuron toxicity. 5'-FUrd showed partial rescue of $SOD1^{WT}$ axonopathy at a 1.5 μM dose (Fig. 5A), however higher doses caused adverse effects in uninjected embryos (Supplemental Fig. 1). In contrast, application of uridine or telbivudine showed no adverse effects on survival nor increase in axonopathy compared to vehicle controls. However for TEER, higher doses of uridine or telbivudine did reduce performance in uninjected embryos compared to untreated embryos (differences in TEER between uridine/telbivudine treated embryos and 0.2% DMSO vehicle controls were not significant for most doses) (Supplemental Fig. 1). In $SOD1^{WT}$ injected embryos, uridine had a more dramatic rescue than 5'-FUrd, producing significant measurable benefits starting at a 0.5 μM dose, in both axonopathy (45% reduction) (Fig. 5A) and TEER performance (24% longer average distance) (Fig. 5B) in $SOD1^{WT}$ injected embryos. Uridine treated $SOD1^{WT}$-injected embryos showed no significant difference from mRNA controls, and a significant rescue from $SOD1^{WT}$ injected embryos treated with DMSO alone ($p < .01$) (Fig. 5A, B). However application of higher doses of uridine (5 μM) decreased TEER performance, so uridine may also have an upper limit of efficacy, at least as measured by the TEER assay. Telbivudine similarly rescued axonopathy in $SOD1^{WT}$ injected embryos at and above established therapeutic doses (Zhou et al., 2006) (41%, 60%, 55%, 57%, and 82% reduction at 1 μg/mL [4.1 μM], 5 μg/mL [20.6 μM], and 10 μg/mL [41.3 μM] doses respectively) ($p < .01$) (Fig. 5C). Application of telbivudine also rescued $SOD1^{WT}$-injected embryos' TEER starting at a 4.1 μM dose. Interpreting this experiment was somewhat confounded by increased swimming induced by 0.2% DMSO vehicle alone (Fig. 5D), though telbivudine further improved rescue of SOD1 treatment when applied at moderate doses. DMSO is included as a vehicle in this assay, as is common in many zebrafish experiments assessing or discovering drugs, largely to improve penetration of drugs into the larval tissues. To further assess this we repeated injections of $SOD1^{WT}$ and assessed telbivudine rescue experiments without DMSO. In axonopathy, the highest dose of telbivudine, 41.3 μM, provided a significant rescue, and a mild rescue was found in TEER at 20.6 μM and 41.3 μM (TEER in these groups were statistically similar to control mRNA injected values, but also not significantly higher than $SOD1^{WT}$ without telbivudine) (Supplemental Fig. 2). Therefore telbivudine is able to reduce SOD1 phenotypes in absence of DMSO.

Furthermore, telbivudine also rescued both axonopathy and TEER induced by a disease-associated variant, $SOD1^{G127X}$, at least at higher doses (20.6 μM and 41.3 μM) (Fig. 5E, F). Telbivudine did not measurably impact the abundance of SOD1 protein (Supplemental Fig. 3).

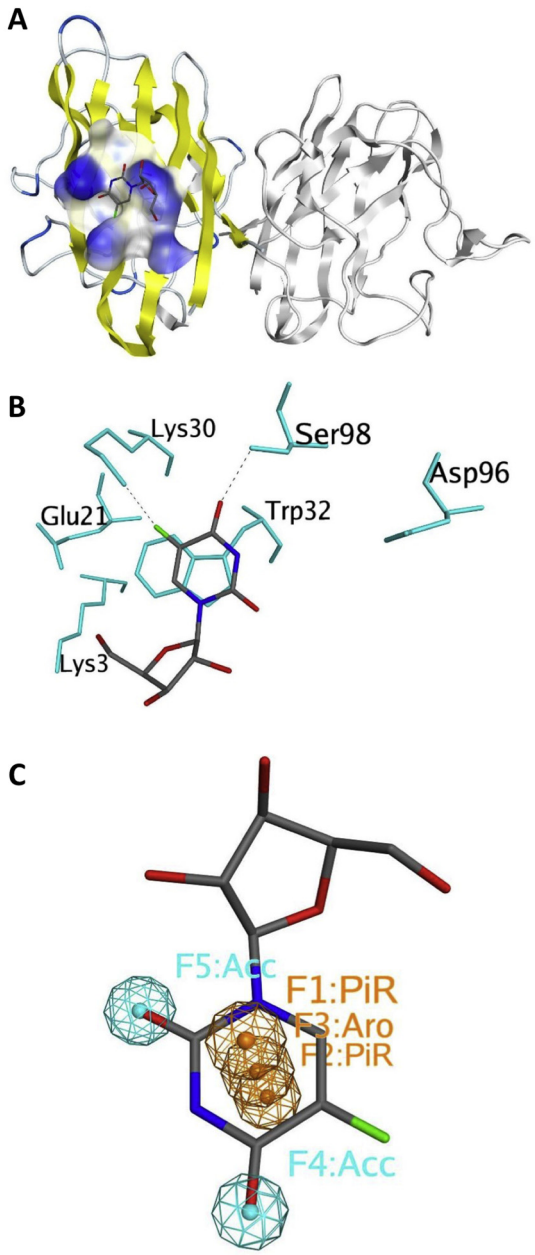

Fig. 3. Experimental binding mode of 5-fluorouridine (5-FUrd) at SOD1, and molecular features of 5-FUrd-based pharmacophore model. A. SOD1 dimer complexed with 5-FUrd from the X-ray structure of human I113T SOD1 mutant co-crystalized with 5-FUrd (PDB accession code: 4A7S). SOD1 is shown in cartoon representation with the first monomer from the 4A7S structure colored according to secondary structure. Solvent exposed surface of residues in the W32 biding site is shown with colors corresponding to the degree of solvent exposure (with blue colour indicating a higher exposure). B. Experimental conformation of 5-FUrd in the W32 binding site of the first monomer from the 4A7S structure. The ligand is colored according to its atom types and residues from the binding site are shown in blue. C. Pharmacophore model built based on the molecular features of the 5-fluorouracil moiety of 5-FUrd. These features include hydrogen bond acceptor atoms (from 4, 2 dioxy groups of uracil shown in cyan) and aromatic pyrimidine ring (highlighted in orange). (For interpretation of the references to colour in this figure legend, the reader is referred to the web version of this article.)

3.3. The actions of telbivudine are via SOD1 and require the W32 residue

To assess if telbivudine acts to mitigate axonopathy specifically via blocking the effects of SOD1, or is instead alleviating neuromuscular

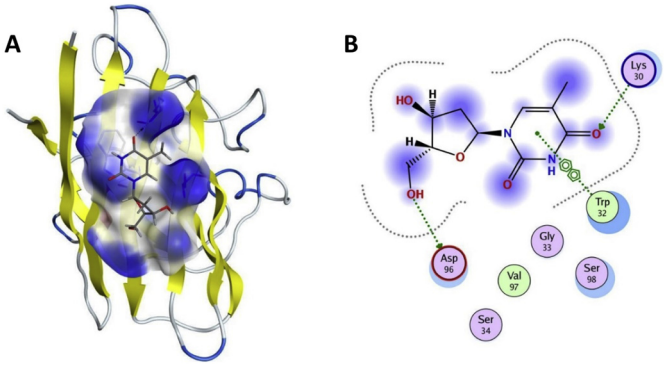

Fig. 4. Probable binding mode of telbivudine at the W32 binding site of SOD1 predicted with combined high throughput virtual screening (HTVS)/pharmacophore screening. A. SOD1 monomer complexed with telbivudine. B. 2-D interaction map of telbivudine and the receptor.

defects in a more general way, we applied telbivudine to other established models of neuromuscular disruption. We confirmed past studies showing that motor neuron axonopathy is significantly induced (Fig. 6) by low doses of ethanol (Shan et al., 2015; Sylvain et al., 2010), and by delivery of a mRNA encoding a disease variant of human ubiquilin 4 (*UBQLN4*^{D90A}) that is causal of ALS (Edens et al., 2017). Telbivudine treatment did not significantly impact the axonopathy induced by either ethanol or ubiquilin 4 (Fig. 6). The actions of telbivudine reducing neuromuscular deficits appear to be centered on SOD1, consistent with its predicted binding to SOD1 described above (Fig. 4).

To ascertain whether the rescue effects of these drugs act via SOD1 and by binding at residue W32 as predicted, or if they mediate some other more general protective mechanism, we applied effective doses of each drug (1.5 μM 5'-FUrd, 1.0 μM uridine, and 20.6 μM telbivudine) to embryos injected with a high dose (1800 pg) of SOD1^{W32S}. We predicted that if 5'-FUrd, uridine, or telbivudine contribute significantly to a neuroprotective mechanism that is independent of the human SOD1 W32 residue, then their protective effects would be additive with the protective effects of the W32S substitution. We observed that applying neither 5'-FUrd, uridine, nor telbivudine had any apparent impact on embryos injected with 1800 pg of SOD1^{W32S} - the resulting axonopathy was unchanged (Fig. 6A). The W32 residue is thus required for these uracil-like nucleoside compounds to exhibit their treatment effects on human SOD1.

These compounds therefore likely do not have generalized neuroprotective effects, but rather have a shared mechanism to protect neurons, such as stabilizing the SOD1 structure via W32 or disrupting aberrant intermolecular interactions that require this solvent-exposed tryptophan residue.

3.4. W32 alone is not sufficient to induce inert species of SOD1 to become toxic

Considering the data above where both gene editing and drug treatments demonstrated that W32 is *necessary* for SOD1 toxicity, and considering the limited occurrence of a Trp residue in this region of SOD1 across taxa (Fig. 1A), we next queried whether W32 is *sufficient* to cause SOD1 toxicity. We tested this by engineering a variant where tryptophan was introduced into the homologous position of zebrafish SOD1. Delivery of this zfSod1^{T33W} variant did not show increased toxicity compared to delivery of wild type zebrafish SOD1 (Fig. 7). This approach was extended to also edit the mouse SOD1 protein, and delivery of the muSOD1^{S33W} variant did not show increased toxicity compared to delivery of wild type mouse SOD1 (Fig. 7). Hence, introduction of a lone tryptophan in these SOD1 proteins was not sufficient to increase the toxic character of SOD1 as measured by axonopathy and TEER. The residue W32 appears to be necessary but not

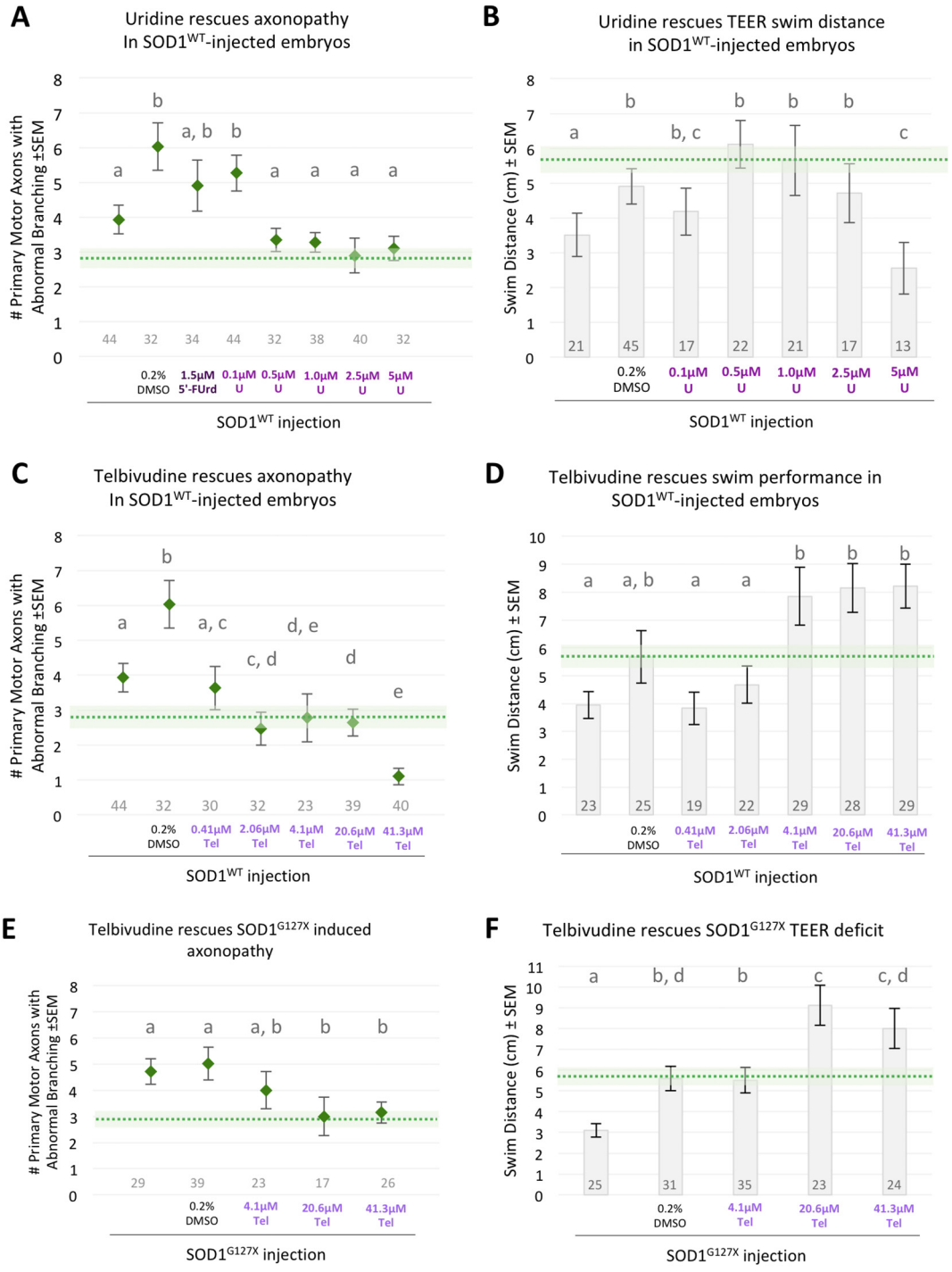

Fig. 5. Uridine and telbivudine decrease SOD1 toxicity and likely act through the W32 residue. A. 5′-fluorouridine (5'-FUrd) (dark purple) partially rescues axonopathy. Uridine (U, bright purple/magenta on x-axis) reduces axonopathy in embryos injected with $SOD1^{WT}$ to control mRNA levels (green dotted line with SEM in green shading), starting at a 0.5 μM dose. B. Uridine (U) also rescues TEER performance in $SOD1^{WT}$-injected embryos back to control mRNA distances (green dotted line with SEM in green shading), in a dose-responsive manner, with greatest rescue at 0.5 μM dose. The TEER group with the highest U dose, 5 μM, performed less well, suggesting an upper limit for uridine exposure. C. Telbivudine (Tel, light purple) similarly reduces axonopathy from $SOD1^{WT}$ at the following doses: 4.1 μM (1 μg/mL), 20.6 μM (5 μg/mL), 41.3 μM (10 μg/mL). Data for $SOD1^{WT}$ and $SOD1^{WT}$ + 0.2% DMSO is re-plotted from [A]. D. Telbivudine rescues TEER from $SOD1^{WT}$ at the following doses: 4.1 μM (1 μg/mL), 20.6 μM (5 μg/mL), 41.3 μM (10 μg/mL). TEER average ± SEM for control mRNA +0.2% DMSO shown. E. Telbivudine rescued axonopathy induced by $SOD1^{G127X}$ at doses 20.6 μM (5 μg/mL) and 41.3 μM (10 μg/mL). F. Telbivudine rescued TEER performance in $SOD1^{G127X}$ injected embryos at 20.6 μM (5 μg/mL) and 41.3 μM (10 μg/mL) (Kruskall-Wallis test with Mann-Whitney pairwise comparisons). TEER average ± SEM for control mRNA +0.2% DMSO shown. mRNA control average ± SEM for each experiment indicated as green dotted line and shaded box. Data values that share matching grey letters within a figure panel are not significantly different. Embryo sample sizes noted below data points. (For interpretation of the references to colour in this figure legend, the reader is referred to the web version of this article.)

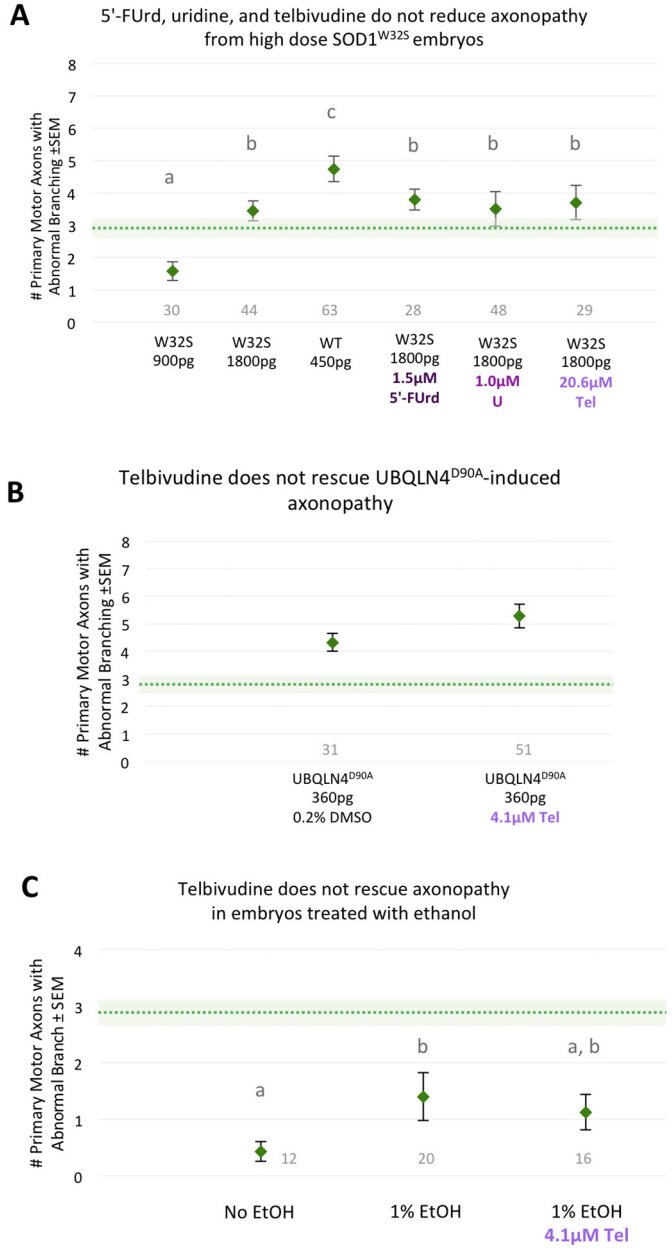

Fig. 6. The actions of telbivudine are via SOD1 and require the W32 residue. A. To determine whether the candidate small molecules exert their rescue effects via the tryptophan residue W32 on SOD1, 5'-FUrd, uridine, or telbivudine at effective doses were applied to SOD1^{W32S} (1800 pg)-injected embryos to test whether they would rescue the mild axonopathy. None of the drugs caused a change in axonopathy, suggesting that these small molecules and W32S act in similar mechanisms to confer protection to motor neurons. (Kruskall-Wallis ANOVA with Mann-Whitney pairwise comparisons, $p < .05$; data from Fig. 2B included here for ease of comparison).). B. UBQLN4^{D90A} caused significant axonopathy above control mRNA levels, and this is not rescued by telbivudine (Mann-Whitney pairwise comparisons, $p = .003$ and $p = 3.33 \times 10^{-5}$ versus control mRNA group, respectively). C. EtOH significantly induced axonopathy and this was not significantly rescued by telbivudine (Mann-Whitney pairwise comparison, $p = .43$). mRNA control average ± SEM for each experiment indicated as green dotted line and shaded box. Data values that share matching grey letters within a figure panel are not significantly different. All drug solutions included 0.2% DMSO. Embryo sample sizes noted below data points. (For interpretation of the references to colour in this figure legend, the reader is referred to the web version of this article.)

sufficient for human SOD1 toxicity, such that the toxicity of human SOD1 may require W32 along with additional residues that are yet to be revealed.

4. Discussion

The conversion of SOD1 from a natively folded to a misfolded conformation is central to the initiation of ALS pathology in SOD1 mutation-associated (fALS) disease, and likely in non-SOD1 associated fALS and sporadic disease as well. What universal domain, residue, or interaction is minimally sufficient (and therefore therapeutically targetable) for both mutant and wildtype SOD1 to acquire toxicity has remained ambiguous. Here we deployed an in vivo model to assess the impacts of a proposed mediator of SOD1 toxicity. We demonstrated that the impacts of human SOD1 on motor neuron axons and motor outputs require the tryptophan in the human SOD1 protein, W32, and these deficits can be specifically ameliorated by drugs targeting this residue.

The SOD1 W32 residue is an intriguing target due to its solvent exposure despite having a hydrophobic side chain. Because selection has maintained this seemingly odd configuration, at least within primates, it would seem that W32S could be mediating or participating in some important aspect of SOD1 biology. Previous mapping to determine which domains drive SOD1 conversion suggested residues 24–36; within this region W32 and its adjacent residues are predicted to form a structure unique to human SOD1, correlating perfectly with a contrast to mouse SOD1, that is not readily converted to a misfolded state (Grad et al., 2011). The presence of this tryptophan may simply increase the probability of conversion (suspected to occur via oxidation of W32 (Coelho et al., 2014; Taylor et al., 2007)), or it may exert conversion effects on neighbouring SOD1 proteins (Grad et al., 2011). For example, the lack of a tryptophan in murine SOD1, and lack of murine SOD1 participation in conversion and aggregation, would support the former hypothesis. In experiments done by Grad et al. (2011), transfection of mouse N2a cells with human SOD1^{G127X} failed to generate detectable misfolded protein. In other words, SOD1^{G127X} had failed to convert mouse SOD1 protein. The presence of a W32 may thus contribute to a SOD1 protein's propensity to be "convertible". However double mutant experiments suggest the latter- that human SOD1^{G127X} and SOD1^{G85R} require a tryptophan at residue 32 to convert SOD1^{WT}. HEK-293 cells transfected with SOD1^{W32S}, SOD1$^{G127X/W32S}$, or SOD1$^{G85R/W32S}$ had produced less signal for misfolded protein compared to their W32-containing counterparts (Grad et al., 2011). Thus to date there is evidence of both roles: tryptophan may increase the probability of conversion within a monomer, and/or it may participate in the conversion of another SOD1 monomer. In this paper we extended the investigation of W32 to whether it is important in SOD1 toxic gain of function in vivo. Using a model amenable to investigations of numerous SOD1 mutants and for screening candidate small molecules, we found that W32 indeed contributes to SOD1 toxicity to motor axon growth and neuromuscular function.

Interestingly, the introduction of a tryptophan residue into SOD1 sequences of other species (mouse and zebrafish SOD1 tested here) alone was not sufficient to impart toxicity. Further work will be required to determine if additional key residue differences between human SOD1 and SOD1 of other species can explain the acquisition of toxicity seen in human SOD1 in neuromuscular disease. Future work could prioritize testing residues that are in close proximity to W32 and that are different between mouse and human SOD1. Considering the primary sequence, there indeed are several adjacent residues (e.g. among residues 30–36, see Fig. 1) that differ between mouse and human SOD1 that might be predicted to impact the biochemical environment surrounding W32. Curiously, this same region shows greater similarity between zebrafish and human SOD1; because our data suggest that zfSOD1^{T33W} exhibits little toxicity this data will influence future efforts to define which residue(s) cooperate with W32 in forming toxic SOD1. This future work might consider residues further afield in

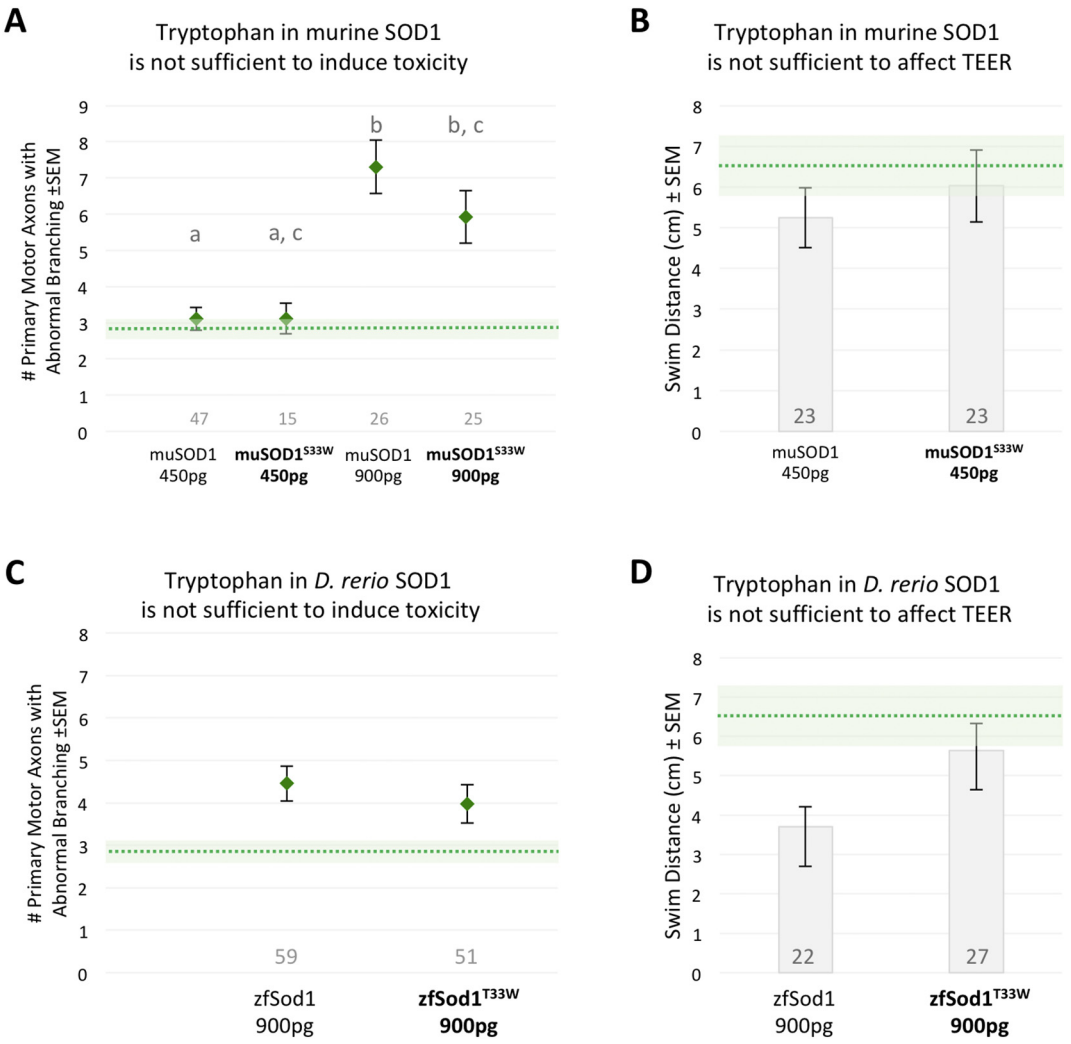

Fig. 7. Introduction of W32 into murine or zebrafish SOD1 proteins is not sufficient to induce toxicity. After defining that W32 is necessary for human SOD1 toxicity, we tested if W32 is sufficient to induce toxic character in SOD1. Tryptophan was substituted into the homologous positions of mouse (murine) and zebrafish SOD1 peptide sequences (creating muSOD1^{S33W} and zfSod1^{T33W} respectively). In axonopathy and TEER assays, introducing tryptophan did not increase the toxicity of either murine [A, B] or zebrafish [C, D] SOD1 proteins (Kruskall-Wallis test and Mann-Whitney *U* tests, $p < .05$). Control mRNA average ± SEM for each experiment indicated as green dotted line and shaded box. Data values that share matching grey letters are not significantly different. Embryo sample sizes noted below data points. (For interpretation of the references to colour in this figure legend, the reader is referred to the web version of this article.)

SOD1, perhaps in several other regions where zebrafish SOD1 has primary sequence that is divergent from the human and mouse (e.g. top of Fig. 1A).

ALS is a multigenic disease, featuring genetic mutations in critical cell processes such as mitochondrial homeostasis, RNA metabolism, and neuromuscular junction support and function (Corcia et al., 2017). Whether misfolded SOD1 has a central role in all these varieties of ALS pathophysiology remains inconclusive, but protein misfolding, mislocalization, and disruption to proteostasis is a prominent theme among mutations in SOD1, TDP43, and FUS (Ayers et al., 2016; Blokhuis et al., 2013; Cashman et al., 2012; Farg et al., 2012; Farrawell et al., 2015; Fushimi et al., 2011; Huang et al., 2011; King et al., 2013; Kwiatkowski et al., 2009; Magrane et al., 2014; Newell et al., 2015; Nordlund et al., 2009; Parakh and Atkin, 2016; Pokrishevsky et al., 2012; Rabdano et al., 2017; Shiihashi et al., 2016; Takanashi and Yamaguchi, 2014; Wang et al., 2013). Protein misfolding is therefore requisite for initiating downstream pathology. Not only can protein misfolding disrupt proteostasis and confer a toxic gain of function, loss-of-function phenotypes are often observed (Allison et al., 2017). Numerous mutations (185 and counting) have been found in the SOD1 gene in patients, but evidence exists that mutation is not required for SOD1 to become toxic (Bosco et al., 2011; Brotherton et al., 2012; Forsberg et al., 2010; Grad et al., 2011; Graffmo et al., 2013; Pokrishevsky et al., 2012). There are biochemical qualities or interactions of SOD1 that enable dimer and/or monomer destabilization and possibly template-directed misfolding, despite the considerable stability of the SOD1 dimer (Malinowski and Fridovich, 1979). The W32 residue unique to primates may be one of the factors that exert destabilizing effects on SOD1. W32 is located in the fairly well conserved (among primates; see Fig. 1A) sequence for β strand 3; selection pressure on this domain within primates may have lead to retention of the W32 residue despite its suspected destabilizing properties (Dasmeh and Kepp, 2017). There are no known human mutations altering the W32 residue specifically, so this tryptophan can be considered nearly universally present in familial and sporadic ALS cases. If tryptophan is indeed a modulator of SOD1 misfolding and toxicity, it could be an attractive treatment target for all ALS patients.

As found in our experiments, adding candidate small compounds to embryos treated with SOD1^{W32S}, UBQLN4^{D90A}, or EtOH (Fig. 6) and our survival data (Supplementary Fig. 1), uridine and telbivudine tested herein do not increase general (neuromuscular) health, but rescue motor neurons by specifically blocking wild-type SOD1 from exerting toxicity. Telbivudine in particular has many optimal qualities of a

candidate therapeutic. As an FDA approved drug currently in use, with a documented and favourable safety profile, it is an example of the promise in evaluating existing drugs for novel applications. We found that the phenotypes measured, axonopathy and TEER, were rescued by different interventions that disrupt this mediator, W32, which is possibly critical to inter-molecular conversion (Grad et al., 2011). Therefore these phenotypes respond with specificity to both the effects of human SOD1 expression and interventions that change SOD1 protein toxicity, an important addition to W32's previously shown role in SOD1 misfolding (Grad et al., 2011). These studies by ourselves and colleagues also further implicate the W32 residue as a mediator of prion-like spread of ALS disease (Grad et al., 2011; Taylor et al., 2007; Pokrishevsky et al., 2018).

Seeking to understand how mutations affect SOD1 stability or toxicity, and selecting compounds to reduce these, are far from new (Alemasov et al., 2017; Anzai et al., 2017; Broom et al., 2015; Das and Plotkin, 2013; Kumar et al., 2017; McAlary et al., 2016; Sekhar et al., 2016; Wright et al., 2013), and most efforts have focused on stabilizing the SOD1 dimer, particularly at the dimer interface. Stabilizing dimers would reduce the frequency of monomerization, which can be considered a rate-limiting step in the spread of SOD1 misfolding and subsequent toxic gain of function (Broom et al., 2015; McAlary et al., 2016; Petrov et al., 2016; Proctor et al., 2016). But combining dimer-stabilizing compounds with complementary ones that can stabilize the protein at other regions may greatly increase therapeutic efficacy while also reducing the required dose of either compound, which is attractive for drugs that may have undesirable side effects at higher doses. The location of W32 results in a flat and unconventional ligand target; however pharmacophore modeling to predict compound-target interactions has provided exciting results in our animal model that await validation in mammalian ALS models.

5. Conclusions

The tryptophan at residue 32 of human SOD1 is unique evolutionarily (unique to primates), and unique within the SOD1 amino acid sequence. Strikingly, modifying W32 in cell culture dramatically reduces SOD1 aggregation and toxicity, and in our animal model it reduces toxicity to motor axons and motor neuron function. Further investigation into how this tryptophan contributes to SOD1 structure, stability, and capacity to become toxic compared to more conserved residues would reveal new insights into SOD1 folding, unfolding, misfolding, and pathological behaviours. The W32 is a promising drug target for preventing SOD1 toxicity, thereby reducing its contribution to debilitating motor neuron degeneration. Indeed deploying that framework led us to identify the nucleoside telbivudine, an FDA-approved drug with good safety profile, for off-target use as a potential drug to ameliorate ALS.

Supplementary data to this article can be found online at https://doi.org/10.1016/j.nbd.2018.11.025.

Ethics approval and consent to participate

Use of animals for this study under the protocol AUP00000077 (University of Alberta) was approved by the Animal Care and Use Committee: BioSciences under the auspices of the Canadian Council on Animal Care. This study did not involve human participants, human data or human tissue.

Authors' contributions

MGD conceived of, performed, statistically analyzed, interpreted and presented all experiments involving zebrafish or drug applications, prioritized drugs to be tested, and was the principal author responsible for drafting the manuscript. VKH conceived of, designed, performed, analyzed and interpreted computational experiments, and wrote the associated portions of the manuscript. NB conceived of, designed, analyzed and interpreted computational experiments, and wrote the associated portions of the manuscript. NS performed and interpreted TEER experiments. RK performed and analyzed Western blot experiments. JB performed and interpreted TEER experiments and performed axonopathy experiments and drug application. EP and NRC conceived of residue W32 being a potential therapeutic target and suggested experiments. AK wrote portions of the manuscript associated with computational experiments. WTA conceived of the experiments, interpreted data and participated in writing the manuscript. AK, NB, and WTA supervised, coordinated and funded the work. All authors read, edited and approved the final manuscript.

Acknowledgements

Technical assistance was provided by Hao Wang and Gavin Neil, and animal care was supported by Xinyue Zhang. UBQLN4 constructs were kindly gifted by Yongchao Ma. Discussions of earlier versions of this manuscript were provided by Steven Plotkin.

Funding

MGD was funded by CIHR and Alberta Innovates Health Solutions MD/PhD awards; operating funds to WTA were in the form of donations; donors had no role in study design. VKH, NB and AK acknowledge the financial support from the Alberta Prion Research Institute (Research team program ABIBS APRIRTP 201300023 and explorations program ABIBS APRIEP 201600034). VKH, NB and AK acknowledge our industrial collaborator, Chemical Computing Group (CCG), for generous support to access their Molecular Operating Environment (MOE) drug discovery software platform. Computational resources were provided by WestGrid (www.westgrid.ca) and Compute/Calcul Canada (www.computecanada.ca). EP and NRC received funding from the Howard Webster Foundation and ALS Canada. No funding body played a role in the design of the study and collection, analysis, and interpretation of data, nor in writing the manuscript.

References

Alemasov, N.A., et al., 2017. Dynamic properties of SOD1 mutants can predict survival time of patients carrying familial amyotrophic lateral sclerosis. J. Biomol. Struct. Dyn. 35, 645–656.
Allison, W.T., et al., 2017. Reduced abundance and subverted functions of proteins in prion-like diseases: gained functions fascinate but lost functions affect aetiology. Int. J. Mol. Sci. 18.
Andersen, P.M., et al., 1997. Phenotypic heterogeneity in motor neuron disease patients with CuZn-superoxide dismutase mutations in Scandinavia. Brain 120, 1723–1737.
Anzai, I., et al., 2017. A misfolded dimer of Cu/Zn-superoxide dismutase leading to pathological oligomerization in amyotrophic lateral sclerosis. Protein Sci. 26, 484–496.
Armstrong, G.A., Drapeau, P., 2013. Loss and gain of FUS function impair neuromuscular synaptic transmission in a genetic model of ALS. Hum. Mol. Genet. 22, 4282–4292.
Ayers, J.I., et al., 2016. Prion-like propagation of mutant SOD1 misfolding and motor neuron disease spread along neuroanatomical pathways. Acta Neuropathol. 131, 103–114.
Banci, L., et al., 2008. SOD1 and Amyotrophic Lateral Sclerosis: Mutations and Oligomerization. PLoS One 3.
Banerjee, V., et al., 2016. Superoxide Dismutase 1 (SOD1)-Derived Peptide Inhibits Amyloid Aggregation of Familial Amyotrophic Lateral Sclerosis SOD1 Mutants. ACS Chem. Neurosci. 7, 1595–1606.
Bidhendi, E.E., et al., 2016. Two superoxide dismutase prion strains transmit amyotrophic lateral sclerosis-like disease. J. Clin. Invest. 126, 2249–2253.
Blokhuis, A.M., et al., 2013. Protein aggregation in amyotrophic lateral sclerosis. Acta Neuropathol. 125, 777–794.
Bosco, D.A., et al., 2011. Proteostasis and Movement Disorders: Parkinson's Disease and Amyotrophic Lateral Sclerosis. Cold Spring Harb. Perspect. Biol. 3.
Bridges, E.G., et al., 2008. Nonclinical safety profile of telbivudine, a novel potent antiviral agent for treatment of hepatitis B. Antimicrob. Agents Chemother. 52, 2521–2528.
Broom, H.R., et al., 2015. Destabilization of the dimer interface is a common consequence of diverse ALS-associated mutations in metal free SOD1. Protein Sci. 24, 2081–2089.
Brotherton, T.E., et al., 2012. Localization of a toxic form of superoxide dismutase 1 protein to pathologically affected tissues in familial ALS. In: Proceedings of the National Academy of Sciences of the United States of America. vol. 109. pp. 5505–5510.

Brown, R.H., 1993. Mutations in Cu/Zn superoxide-dismutase (Sod1) are associated with familial amyotrophic-lateral-sclerosis (Als). Free Radic. Biol. Med. 15, 471.
Bruijn, L.I., et al., 1997. ALS-linked SOD1 mutant G85R mediates damage to astrocytes and promotes rapidly progressive disease with SOD1-containing inclusions. Neuron 18, 327–338.
Bruijn, L.I., et al., 1998. Aggregation and motor neuron toxicity of an ALS-linked SOD1 mutant independent from wild-type SOD1. Science 281, 1851–1854.
Case, D.A., III, CheathamTE, Simmerling, C.L., Wang, J., Duke, R.E., Luo, R., MRCW, Crowley, Walker, R.C., Zhang, W., Merz, K.M., Wang, B., Hayik, S., Roitberg, A., Seabra, G., Kolossváry, I., Wong, K.F., Paesani, F., Vanicek, J., Wu, X., Brozell, S.R., Steinbrecher, T., Gohlke, H., Yang, L., Tan, C., Mongan, J., Hornak, V., Cui, G., Mathews, D.H., Seetin, M.G., Sagui, C., Babin, V., Kollman, P.A., 2008. Amber 10. University of California.
Cashman, N., et al., 2012. Propagated misfolding of SOD1 in ALS. Prion 6, 12.
Chia, R., et al., 2010. Superoxide dismutase 1 and tgSOD1(G93A) mouse spinal cord seed fibrils, suggesting a propagative cell death mechanism in amyotrophic lateral sclerosis. PLoS One 5.
Coelho, F.R., et al., 2014. Oxidation of the tryptophan 32 residue of human superoxide dismutase 1 caused by its bicarbonate-dependent peroxidase activity triggers the non-amyloid aggregation of the enzyme. J. Biol. Chem. 289, 30690–30701.
Corcia, P., et al., 2017. Genetics of amyotrophic lateral sclerosis. Rev. Neurol. (Paris) 173, 254–262.
Das, A., Plotkin, S.S., 2013. SOD1 exhibits allosteric frustration to facilitate metal binding affinity. Proc. Natl. Acad. Sci. U. S. A. 110, 3871–3876.
Dasmeh, P., Kepp, K.P., 2017. Superoxide dismutase 1 is positively selected to minimize protein aggregation in great apes. Cell. Mol. Life Sci. 74, 3023–3037.
Deng, H.X., et al., 2006. Conversion to the amyotrophic lateral sclerosis phenotype is associated with intermolecular linked insoluble aggregates of SOD1 in mitochondria. In: Proceedings of the National Academy of Sciences of the United States of America. vol. 103. pp. 7142–7147.
Didonato, M., et al., 2003. ALS mutants of human superoxide dismutase form fibrous aggregates via framework destabilization (vol 332, pg 601, 2003). J. Mol. Biol. 334, 175.
Duval, M.G., et al., 2014. Growth differentiation factor 6 as a putative risk factor in neuromuscular degeneration. PLoS One 9.
Edens, B.M., et al., 2017. A novel ALS-associated variant in UBQLN4 regulates motor axon morphogenesis. elife 6.
Farg, M.A., et al., 2012. Mutant FUS induces endoplasmic reticulum stress in amyotrophic lateral sclerosis and interacts with protein disulfide-isomerase. Neurobiol. Aging 33, 2855–2868.
Farrawell, N.E., et al., 2015. Distinct partitioning of ALS associated TDP-43, FUS and SOD1 mutants into cellular inclusions. Sci. Rep. 5.
Fischer, L.R., et al., 2012. Absence of SOD1 leads to oxidative stress in peripheral nerve and causes a progressive distal motor axonopathy. Exp. Neurol. 233, 163–171.
Forsberg, K., et al., 2010. Novel antibodies reveal inclusions containing non-native SOD1 in sporadic ALS patients. PLoS One 5, e11552.
Fung, J., et al., 2011. Nucleoside/nucleotide analogues in the treatment of chronic hepatitis B. J. Antimicrob. Chemother. 66, 2715–2725.
Furukawa, Y., et al., 2013. Intracellular seeded aggregation of mutant Cu,Zn-superoxide dismutase associated with amyotrophic lateral sclerosis. FEBS Lett. 587, 2500–2505.
Fushimi, K., et al., 2011. Expression of human FUS/TLS in yeast leads to protein aggregation and cytotoxicity, recapitulating key features of FUS proteinopathy. Protein Cell. 2, 141–149.
Gerber, P.R., Muller, K., 1995. Mab, a generally applicable molecular-force field for structure modeling in medicinal chemistry. J. Comput. Aided Mol. Des. 9, 251–268.
Grad, L.I., et al., 2011. Intermolecular transmission of superoxide dismutase 1 misfolding in living cells. In: Proceedings of the National Academy of Sciences of the United States of America. vol. 108. pp. 16398–16403.
Grad, L.I., et al., 2015. From molecule to molecule and cell to cell: prion-like mechanisms in amyotrophic lateral sclerosis. Neurobiol. Dis. 77, 257–265.
Graffmo, K.S., et al., 2013. Expression of wild-type human superoxide dismutase-1 in mice causes amyotrophic lateral sclerosis. Hum. Mol. Genet. 22, 51–60.
Gurney, M.E., et al., 1994. Motor-neuron degeneration in mice that express a human Cu,Zn superoxide-dismutase mutation. Science 264, 1772–1775.
Hansen, C., et al., 1998. Novel 4-bp insertion in exon 5 of the CuZn superoxide dismutase (SOD1) gene associated with familial amyotrophic lateral sclerosis. Hum. Mutat. S327–S328.
Huang, C., et al., 2011. FUS transgenic rats develop the phenotypes of amyotrophic lateral sclerosis and Frontotemporal lobar degeneration. PLoS Genet. 7.
Ivannikov, M.V., Van Remmen, H., 2015. Sod1 gene ablation in adult mice leads to physiological changes at the neuromuscular junction similar to changes that occur in old wild-type mice. Free Radic. Biol. Med. 84, 254–262.
Jaarsma, D., et al., 2008. Neuron-specific expression of mutant superoxide dismutase is sufficient to induce amyotrophic lateral sclerosis in transgenic mice. J. Neurosci. 28, 2075–2088.
Jakalian, A., et al., 2000. Fast, efficient generation of high-quality atomic charges. AM1-BCC model: I. Method. J. Comput. Chem. 21, 132–146.
Jakalian, A., et al., 2002. Fast, efficient generation of high-quality atomic charges. AM1-BCC model: II. Parameterization and validation. J. Comput. Chem. 23, 1623–1641.
Jonsson, P.A., et al., 2004. Minute quantities of misfolded mutant superoxide dismutase-1 cause amyotrophic lateral sclerosis. Brain 127, 73–88.
Jonsson, P.A., et al., 2006. Disulphide-reduced superoxide dismutase-1 in CNS of transgenic amyotrophic lateral sclerosis models. Brain 129, 451–464.
Kabashi, E., et al., 2010. Gain and loss of function of ALS-related mutations of TARDBP (TDP-43) cause motor deficits in vivo. Hum. Mol. Genet. 19, 671–683.
Kabashi, E., et al., 2011. FUS and TARDBP but not SOD1 interact in genetic models of amyotrophic lateral sclerosis. PLoS Genet. 7, e1002214.
Kanyo, R., et al., 2011. Adrenergic regulation of the distribution of transducer of regulated camp-response element-binding protein (TORC2) in rat pinealocytes. Endocrinology 152, 3440–3450.
Khan, M.A.I., et al., 2017. Cu/Zn superoxide dismutase forms amyloid fibrils under near physiological quiescent conditions: the roles of disulfide bonds and effects of denaturant. ACS Chem. Neurosci. 8, 2019–2026.
King, A., et al., 2013. Mixed tau, TDP-43 and p62 pathology in FTLD associated with a C9ORF72 repeat expansion and p.Ala239Thr MAPT (tau) variant. Acta Neuropathol. 125, 303–310.
Kumar, V., et al., 2017. Computing disease-linked SOD1 mutations: deciphering protein stability and patient-phenotype relations. Sci. Rep. 7.
Kwiatkowski, T.J., et al., 2009. Mutations in the FUS/TLS gene on chromosome 16 cause familial amyotrophic lateral sclerosis. Science 323, 1205–1208.
Lemmens, R., et al., 2007. Overexpression of mutant superoxide dismutase 1 causes a motor axonopathy in the zebrafish. Hum. Mol. Genet. 16, 2359–2365.
Magrane, J., et al., 2014. Abnormal mitochondrial transport and morphology are common pathological denominators in SOD1 and TDP43 ALS mouse models. Hum. Mol. Genet. 23, 1413–1424.
Malinowski, D.P., Fridovich, I., 1979. Subunit association and side-chain reactivities of bovine erythrocyte superoxide-dismutase in denaturing solvents. Biochemistry 18, 5055–5060.
McAlary, L., et al., 2016. Susceptibility of mutant SOD1 to form a destabilized monomer predicts cellular aggregation and toxicity but not in vitro aggregation propensity. Front. Neurosci. 10, 499.
Molecular Operating Environment (MOE), 2013. Chemical Computing Group ULC, 1010 Sherbrooke St. West, Suite #910, Montreal, QC, Canada, H3A 2R7, 2018.
Muller, F.L., et al., 2006. Absence of CuZn superoxide dismutase leads to elevated oxidative stress and acceleration of age-dependent skeletal muscle atrophy. Free Radic. Biol. Med. 40, 1993–2004.
Münch, C., Bertolotti, A., 2011. Self-propagation and transmission of misfolded mutant SOD1: Prion or prion-like phenomenon? Cell Cycle 10, 1711.
Newell, K., et al., 2015. Behavioral variant-frontotemporal dementia and parkinson disease associated with tau, alpha-synuclein, and TDP43 neuropathology. J. Neuropathol. Exp. Neurol. 74, 599.
Nordlund, A., et al., 2009. Functional features cause misfolding of the ALS-provoking enzyme SOD1. In: Proceedings of the National Academy of Sciences of the United States of America. vol. 106. pp. 9667–9672.
Nowak, R.J., et al., 2010. Improving binding specificity of pharmacological chaperones that target mutant superoxide dismutase-1 linked to familial amyotrophic lateral sclerosis using computational methods. J. Med. Chem. 53, 2709–2718.
Parakh, S., Atkin, J.D., 2016. Protein folding alterations in amyotrophic lateral sclerosis. Brain Res. 1648, 633–649.
Petrov, D., et al., 2016. Effect of oxidative damage on the stability and dimerization of superoxide dismutase 1. Biophys. J. 110, 1499–1509.
Pokrishevsky, E., McAlary, L., Farrawell, N.E., Zhao, B., Sher, M., Yerbury, J.J., Cashman, NR., 2018 Oct 22. Tryptophan 32-mediated SOD1 aggregation is attenuated by pyrimidine-like compounds in living cells. Sci. Reports 8 (1), 1402. https://doi.org/10.1038/s41598-018-32835-y. (PMID: 30349065).
Pokrishevsky, E., et al., 2012. Aberrant localization of FUS and TDP43 is associated with misfolding of SOD1 in amyotrophic lateral sclerosis. PLoS One 7.
Proctor, E.A., et al., 2016. Nonnative SOD1 trimer is toxic to motor neurons in a model of amyotrophic lateral sclerosis. In: Proceedings of the National Academy of Sciences of the United States of America. vol. 113. pp. 614–619.
Rabdano, S.O., et al., 2017. Onset of disorder and protein aggregation due to oxidation-induced intermolecular disulfide bonds: case study of RRM2 domain from TDP-43. Sci. Rep. 7.
Ramesh, T., et al., 2010. A genetic model of amyotrophic lateral sclerosis in zebrafish displays phenotypic hallmarks of motoneuron disease. Dis. Model. Mech. 3, 652–662.
Ray, S.S., et al., 2005. Small-molecule-mediated stabilization of familial amyotrophic lateral sclerosis-linked superoxide dismutase mutants against unfolding and aggregation. In: Proceedings of the National Academy of Sciences of the United States of America. vol. 102. pp. 3639–3644.
Reaume, A.G., et al., 1996. Motor neurons in Cu/Zn superoxide dismutase-deficient mice develop normally but exhibit enhanced cell death after axonal injury. Nat. Genet. 13, 43–47.
Sakowski, S.A., et al., 2012. Neuromuscular effects of G93A-SOD1 expression in zebrafish. Mol. Neurodegener. 7.
Sasaki, S., et al., 2005. Ultrastructural study of aggregates in the spinal cord of transgenic mice with a G93A mutant SOD1 gene. Acta Neuropathol. 109, 247–255.
Sekhar, A., et al., 2016. Probing the free energy landscapes of ALS disease mutants of SOD1 by NMR spectroscopy. Proc. Natl. Acad. Sci. U. S. A. 113, E6939–E6945.
Shan, S.D., et al., 2015. Ethanol exposure during gastrulation alters neuronal morphology and behavior in zebrafish. Neurotoxicol. Teratol. 48, 18–27.
Shi, Y., et al., 2014. The lack of CuZnSOD leads to impaired neurotransmitter release, neuromuscular junction destabilization and reduced muscle strength in mice. PLoS One 9, e100834.
Shi, Y.H., et al., 2016. Gibbs Energy of Superoxide Dismutase Heterodimerization Accounts for Variable Survival in Amyotrophic Lateral Sclerosis. J. Am. Chem. Soc. 138, 5351–5362.
Shiihashi, G., et al., 2016. Mislocated FUS is sufficient for gain-of-toxic-function amyotrophic lateral sclerosis phenotypes in mice. Brain 139, 2380–2394.
Stathopulos, P.B., et al., 2003. Cu/Zn superoxide dismutase mutants associated with amyotrophic lateral sclerosis show enhanced formation of aggregates in vitro. In: Proceedings of the National Academy of Sciences of the United States of America. vol. 100. pp. 7021–7026.

Sundaramoorthy, V., et al., 2013. Extracellular wildtype and mutant SOD1 induces ER-Golgi pathology characteristic of amyotrophic lateral sclerosis in neuronal cells. Cell. Mol. Life Sci. 70, 4181–4195.
Sylvain, N.J., et al., 2010. Zebrafish embryos exposed to alcohol undergo abnormal development of motor neurons and muscle fibers. Neurotoxicol. Teratol. 32, 472–480.
Takanashi, K., Yamaguchi, A., 2014. Aggregation of ALS-linked FUS mutant sequesters RNA binding proteins and impairs RNA granules formation. Biochem. Biophys. Res. Commun. 452, 600–607.
Taylor, D.M., et al., 2007. Tryptophan 32 potentiates aggregation and cytotoxicity of a copper/zinc superoxide dismutase mutant associated with familial amyotrophic lateral sclerosis. J. Biol. Chem. 282, 16329–16335.
Wang, J., et al., 2002. Fibrillar inclusions and motor neuron degeneration in transgenic mice expressing superoxide dismutase 1 with a disrupted copper-binding site. Neurobiol. Dis. 10, 128–138.
Wang, L.J., et al., 2009. Wild-type SOD1 overexpression accelerates disease onset of a G85R SOD1 mouse. Hum. Mol. Genet. 18, 1642–1651.
Wang, I.F., et al., 2013. Autophagy activation ameliorates neuronal pathogenesis of FTLD-U mice: a new light for treatment of TARDBP/TDP-43 proteinopathies. Autophagy 9, 239–240.
Westerfield, M., 2000. The zebrafish book. A guide for the laboratory use of zebrafish (*Danio rerio*). University of Oregon Press, Eugene, OR 97403.
Wishart, D.S., et al., 2006. DrugBank: a comprehensive resource for in silico drug discovery and exploration. Nucleic Acids Res. 34, D668–D672.
Wong, P.C., et al., 1995. An adverse Property of a Familial Als-Linked Sod1 Mutation Causes Motor-Neuron Disease Characterized by Vacuolar Degeneration of Mitochondria. Neuron 14, 1105–1116.
Wright, G.S.A., et al., 2013. Ligand binding and aggregation of pathogenic SOD1. Nat. Commun. 4.
Yamagishi, S., et al., 2007. An in Vitro model for lewy body-like hyaline inclusion/astrocytic hyaline inclusion: induction by ER stress with an ALS-linked SOD1 mutation. PLoS One 2.
Zhang, X.S., et al., 2008. Clinical features of adverse reactions associated with telbivudine. World J. Gastroenterol. 14, 3549–3553.
Zhou, X.J., et al., 2006. Pharmacokinetics of telbivudine in healthy subjects and absence of drug interaction with lamivudine or adefovir dipivoxil. Antimicrob. Agents Chemother. 50, 2309–2315.